Robust Solution of Richards' Equation for Non-Uniform Porous Media

Cass T. Miller and Glenn A. Williams
Department of Environmental Sciences and Engineering, University of North Carolina,

Chapel Hill, NC

C. T. Kelley and Michael D. Tocci
Department of Mathematics, North Carolina State University, Raleigh, NC

Short title: ROBUST SOLUTION OF RICHARDS' EQUATION

Abstract. Capillary pressure-saturation-relative permeability relations described using the van Genuchten and Mualem models for non-uniform porous media lead to numerical convergence difficulties when used with Richards' equation for certain auxiliary conditions. These difficulties arise because of discontinuities in the derivative of specific moisture capacity and relative permeability as a function of capillary pressure. Convergence difficulties are illustrated using standard numerical approaches to simulate such problems. Constitutive relations, interblock permeability, and nonlinear algebraic system approximation methods, and two time integration approaches are investigated. An integral permeability approach approximated by Hermite polynomials is recommended and shown to be robust and economical for a set of test problems, which correspond to a sand, a loam, and a clay loam media.

1. Introduction

Fluid flow in unsaturated porous media is often modeled using Richards' equation (RE) [*Richards,* 1931] and closed by constitutive relations to describe the relationship among fluid pressures, saturations, and relative permeabilities [*Brooks and Corey,* 1966; *van Genuchten,* 1980]. Because of the nonlinearities involved, RE is often solved using low-order numerical approximation methods, such as finite difference or finite element methods. These types of solution methods are used in many of the existing unsaturated flow codes. The application of these codes to a wide variety of problems is considered commonplace [*van der Heidje,* 1996]. The standard use of such simulation methods notwithstanding, problems exist with both the robustness and efficiency of numerical solutions to RE; advancements in the solution of these problems is an important and active topic of research in the water resources community.

A common set of constitutive relations used to close RE is the van Genuchten relation to describe the interdependence of fluid pressures and saturations and the Mualem relation to describe the interdependence between fluid saturation and relative permeability. The exponent, or n_v, in the van Genuchten relation is a measure of pore-size uniformity. For many natural porous media, typical values of n_v range between 1.0 to 2.0, when determined using standard laboratory approaches and fitted using standard inverse techniques [*Kool et al.,* 1985; *van Genuchten et al.,* 1991].

Using the van Genuchten and Mualem (VGM) constitutive relations in existing RE codes, we experienced significant problems in attaining a convergent solution for cases in which $n_v < 2$ for certain sets of auxiliary conditions. An example of such a case was for infiltration from a ponded surface boundary condition into a system originally drained to equilibrium.

These experiences motivated this work, which had several objectives: (1) to document a common class of variably-saturated flow problems that lack robustness when solved using standard solution approaches; (2) to determine the reason why traditional

approaches lack robustness for this class of problems; (3) to investigate a variety of alternative approaches; and (4) to compare a set of alternative approaches for a range of media conditions to test robustness and efficiency.

2. Background

Four aspects of the literature on unsaturated flow warrant at least a brief consideration: (1) constitutive relations used to describe pressure-saturation-conductivity relations and typical parameter values for natural, unconsolidated media; (2) approaches typically used to approximate RE; (3) methods for approximating relative permeabilities in a discrete approximation of RE; and (4) strategies used to estimate the relatively complex constitutive relations that are a part of the formulations of concern. We discuss each of these aspects in turn.

2.1. Pressure-Saturation-Conductivity Relations

A well-posed formulation of RE requires that constitutive relations be specified to describe the interdependence among fluid pressures, saturations, and relative permeabilities, which will be referred to as *p-s-k* relations. Several approaches have been advanced to describe *p-s-k* relations [*Brooks and Corey,* 1966; *Mualem,* 1976; *van Genuchten,* 1980], but determining the most appropriate constitutive relation formulation is still an open issue. We use the van Genuchten relation to describe the relationship between fluid pressures and saturations [*van Genuchten,* 1980] and the Mualem relation for that between fluid saturations and relative permeabilities [*Mualem,* 1976]. Several codes documented in the literature use these relations to close RE (e.g., [*Yeh,* 1987; *Simunek and van Genuchten,* 1994]). We will refer to these relations collectively as the van Genuchten/Mualem (VGM) relations.

Because of the widespread use of the van Genuchten relation, many experimental data sets have been described using this approach, and many sets of parameter values

are available in the literature [*van Genuchten et al.,* 1991]. In addition, a parameter estimation code is available and has been widely used to determine these parameter values from experimental data [*van Genuchten et al.,* 1991]. These parameter values are related to the mean pores size (α_v) and the uniformity of the pore-size distribution (n_v).

The standard range of values of n_v is of particular interest; it can vary from near 1.0 [*van Genuchten et al.,* 1991] to near or even greater than 10.0 [*Kool and Parker,* 1987; *Mayer and Miller,* 1992], with the pore size distribution being increasingly uniform as n_v increases. Most natural media tested to date do not have a highly uniform pore-size distribution, so $n_v < 2.0$ for many natural unconsolidated media [*van Genuchten et al.,* 1991]. For such media, the VGM relations are not smooth, which can lead to difficulties in achieving convergence for the common numerical approximation approaches to RE that rely upon these relations [*Vogel and Cislerova,* 1988].

To alleviate this problem, a portion of the functions near the zero pressure head point is often linearized; e.g., a linear function is used to describe the relative permeability for $\psi > \psi_t$, for some $\psi_t < 0.0$. This approach acts to smooth the highly nonlinear functions that are problematic for the nonlinear solver. This approach is used in the popular finite element variably saturated flow code Chain_2D [*Simunek and van Genuchten,* 1994]. Others have used essentially the same approach; for example, the primary variable switching technique [*Forsyth et al.,* 1995] makes use of a similar smoothing technique. This approach may permit more robust convergence of the nonlinear solver in some cases, but robustness problems and solution accuracy issues still remain [*Vogel and Cislerova,* 1988; *Vogel et al.,* 1991].

2.2. Numerical Solutions for Richards' Equation

The nonlinearity of RE, the complex nature of the *p-s-k* relations, including hysteresis [*Scott et al.,* 1984; *Kool and Parker,* 1987; *Lenhard et al.,* 1989], and the

heterogeneous nature of subsurface systems [*Christakos,* 1992; *Gelhar,* 1993] combine to make numerical approximation approaches the most common way of solving RE. Many reports of approximate numerical solutions to RE have appeared in the literature, with low-order finite-difference [*Hanks and Bowers,* 1962; *Rubin,* 1968; *Hornberger and Remson,* 1969; *Cooley,* 1971; *Freeze,* 1971; *Vauclin et al.,* 1979; *Celia et al.,* 1990] and finite-element [*Cooley,* 1983; *Huyakorn et al.,* 1984; *Allen and Murphy,* 1986; *Celia et al.,* 1990] the most common methods. Such solutions to RE are used routinely for applications involving agricultural, geochemical, and nuclear waste-disposal applications [*van der Heidje,* 1996], among others. The robust solution of these applications is desirable, but is not currently possible for certain common sets of constitutive relations, parameter values, and auxiliary conditions.

2.3. Relative Permeability Approximation

Estimating interblock relative permeabilities for grid blocks in the vicinity of saturation is another problem in the numerical simulation of unsaturated/saturated flow in media with $n_v < 2$. In this region, relative permeabilities can vary greatly for a small change in capillary pressure, and convergence of the nonlinear solver is very sensitive to the method used to estimate the interblock relative permeabilities.

In many existing numerical procedures, interblock relative permeability is estimated as the arithmetic average of the two neighboring cells' relative permeabilities [*Haverkamp and Vauclin,* 1979; *Warrick,* 1991; *Zaidel and Russo,* 1992]. This procedure, however, results in an overestimation of interblock permeability and in a significant smearing of the steep wetting front [*Zaidel and Russo,* 1992].

Alternative approaches have been proposed, including geometric mean [*Haverkamp and Vauclin,* 1979; *Zaidel and Russo,* 1992], harmonic mean [*Haverkamp and Vauclin,* 1979], one- and two-point upstream weighting [*Haverkamp and Vauclin,* 1979], a Kirchoff integral method [*Zaidel and Russo,* 1992], and a weighted averaging scheme

based upon matching Darcy fluxes [*Warrick,* 1991]. Some comparisons among methods have been completed [*Zaidel and Russo,* 1992], but general guidance is not yet available.

2.4. Constitutive Relation Estimation

The VGM relations involve complicated power functions that are computationally expensive to evaluate during the course of a simulation [*Ross,* 1992]. To reduce the computational cost, function values are often tabulated and intermediate values required during the simulation are interpolated either by linear or higher-order interpolation. This approach can significantly reduce the overall cost and runtime of an unsaturated flow simulation [*Simunek and van Genuchten,* 1994; *Ross,* 1992].

Cubic spline interpolation is an effective higher-order interpolation approach in which a C^2 continuous interpolation polynomial is constructed so that at each of the spline knots, the value of the polynomial equals the actual function value [*Ross,* 1992] This approach works well for most porous media conditions, yet it is difficult to maintain accuracy using cubic spline interpolation for the VGM relations when $n_v < 2$. Under this condition, the permeability and specific moisture capacity functions become less smooth than when $n_v \geq 2$. When using cubic spline interpolation, second derivatives of the interpolation polynomial at each of the spline knots are computed by solving a system of linear equations whose dimension is equal to the number of spline knots. For this class of problems, significant oscillations can occur in the solution of this system of equations near the non-smooth region of the relation, which in this case occurs near the saturated/unsaturated transition region. These oscillations cause accuracy loss in interpolating intermediate function values and lead ultimately to convergence difficulties for the nonlinear solver.

3. Approach

3.1. Formulation

RE may be formulated several ways [*Huyakorn and Pinder,* 1983; *Milly,* 1985; *deMarsily,* 1986; *Celia et al.,* 1990]. In this work, we examine two temporal discretization methods, each of which uses a different form of RE. The central issues in this work are dependent on neither the form of RE used nor the spatial dimensionality of the problem. For this reason, our formulation and analysis are restricted to one spatial dimension.

A mass-conserving mixed-form of RE is routinely used in research and production codes [*Yeh,* 1987; *Celia et al.,* 1990; *Simunek and van Genuchten,* 1994]. For the case in which fluid compressibility is included for a one-spatial-dimension vertical system, the common mixed-form equation is

$$S_s S_a(\psi)\frac{\partial \psi}{\partial t} + \frac{\partial \theta_a}{\partial t} = \frac{\partial}{\partial z}\left[K_z(\psi)\left(\frac{\partial \psi}{\partial z} + 1\right)\right] \tag{1}$$

where S_s is the specific storage coefficient, which accounts for fluid compressibility; S_a is the saturation of the aqueous phase; ψ is the pressure head; t is time; θ_a is the volumetric water content of the aqueous phase; z is the vertical spatial dimension; and K_z is the hydraulic permeability.

We also use the compressible, pressure-head-based form of RE, which in one spatial dimension may be written as

$$[c(\psi) + S_s S_a(\psi)]\frac{\partial \psi}{\partial t} = \frac{\partial}{\partial z}\left[K_z(\psi)\left(\frac{\partial \psi}{\partial z} + 1\right)\right] \tag{2}$$

where c is the specific moisture capacity. While mass conservation problems using traditional low-order methods with this form of RE are well known [*Celia et al.,* 1990; *Rathfelder and Abriola,* 1994], recent work using higher-order methods in time has shown that solutions of the pressure-head form of the equation can be accurate, robust, and economical [*Tocci et al.,* 1997].

We consider problems with auxiliary conditions of the form

$$\psi(z, t = 0) = \psi_0(z) \tag{3}$$

$$\psi(z = 0, t > 0) = \psi_1 \tag{4}$$

$$\psi(z = Z, t > 0) = \psi_2 \tag{5}$$

where Z is the length of the domain, ψ_0 may be a function of space, and ψ_1 and ψ_2 are constants. We consider these auxiliary conditions because they lead to the development of a sharp infiltration front and saturated conditions over a portion of the domain, which is a difficult class of test problem.

3.2. Constitutive Relations

Solving RE requires constitutive relations to describe the interdependence among fluid pressures, saturations, and relative permeability. The focus of this work is on the often-used van Genuchten (VG) pressure-saturation relationship [*van Genuchten,* 1980], which is given by

$$S_e(\psi) = \frac{\theta_a(\psi) - \theta_r}{\theta_s - \theta_r} = \begin{cases} (1 + |\alpha_v \psi|^{n_v})^{-m_v}, & \psi < 0 \\ 1, & \psi \geq 0 \end{cases} \tag{6}$$

where $m_v = 1 - 1/n_v$, S_e is the effective saturation, θ_r is the residual volumetric water content, θ_s is the saturated volumetric water content, α_v is a parameter related to the mean pore size, and n_v is a parameter related to the uniformity of the pore-size distribution.

Clearly S_e is continuously differentiable at $\psi = 0$ if $1 \leq n_v$. However, if $1 < n_v < 2$, then S_e is not Lipschitz continuously differentiable and the second derivative of S_e is infinite at $\psi = 0$.

The specific moisture capacity, c, is defined as $d\theta_a/d\psi$. Using (6) we see that, for $\psi < 0$,

$$c(\psi) = d\theta_a/d\psi = (\theta_s - \theta_r) S_e'(\psi)$$

$$= \quad (\theta_s - \theta_r) m_v (1 + |\alpha_v \psi|^{n_v})^{-m_v - 1} n_v \alpha_v |\alpha_v \psi|^{n_v - 1}. \tag{7}$$

If $1 < n_v < 2$, then c is not differentiable at $\psi = 0$, and this lack of smoothness will affect the performance of any nonlinear solver.

The saturation-permeability relation is described using Mualem's model for the relative permeability of the aqueous phase [*Mualem,* 1976]

$$K_z(S_e) = K_s S_e^{1/2} \left[1 - \left(1 - S_e^{1/m_v}\right)^{m_v}\right]^2 \tag{8}$$

where K_s is the water-saturated hydraulic permeability, and $S_e = S_e(\psi)$ from (6).

As with c, K_z will lose smoothness for small n_v. In fact, for $\psi < 0$,

$$K_z(\psi) = 1 + O(|\psi|^{m_v n_v}) = 1 + O(|\psi|^{n_v - 1}) \tag{9}$$

as $\psi \to 0$. At $\psi = 0$, K_z' is discontinuous if $n_v = 2$ and infinite if $1 < n_v < 2$.

3.3. Spatial Discretization

We use a standard finite-difference approximation to discretize RE with respect to the spatial dimension [*Celia et al.,* 1990], z, where $z \in [0, Z]$. We consider a uniform spatial discretization comprised of $n_n - 1$ intervals $\{[z_i, z_{i+1}]\}_{i=1}^{n_n - 1}$, of length Δz, with $\Delta z = Z/(n_n - 1)$, and $z_i = (i-1)\Delta z$ for $1 \le i \le n_n$. The spatial operator

$$O_{sd}(\psi) = \frac{\partial}{\partial z}\left[K_z(\psi)\left(\frac{\partial \psi}{\partial z} + 1\right)\right] \tag{10}$$

is approximated at $z = z_i$ for $1 < i < n_n$ by

$$O_{sdi}(\psi) = \Delta z^{-1}\left(\frac{K_{i+1/2}(\psi_{i+1} - \psi_i) - K_{i-1/2}(\psi_i - \psi_{i-1})}{\Delta z} + K_{i+1/2} - K_{i-1/2}\right) \tag{11}$$

where n_n is the number of spatial nodes in the solution, and ψ_i is the approximation to $\psi(z_i)$.

3.4. Temporal Discretization

We investigated two time-integration methods in this work: a standard first-order backward-difference approximation of the mixed-form of RE [*Celia et al.,* 1990], which is given by (1); and a higher-order differential algebraic equation/method of lines (DAE/MOL) approach applied to the ψ-based form of RE [*Tocci et al.,* 1997], which is given by (2).

The mixed-form equation is written in discrete form as

$$S_{si}S_{ai}^{l+1}\frac{\psi_i^{l+1}-\psi_i^l}{\Delta t}+\frac{\theta_{a_i}^{l+1}-\theta_{a_i}^l}{\Delta t}=O_{sdi}(\psi)^{l+1} \tag{12}$$

where l is a time step index representing a known time level, and $l+1$ is an index representing an unknown time level.

For the DAE/MOL approach, the semi-discrete form of the pressure equation is written as

$$A(\psi)_i\frac{d\psi_i}{dt}=O_{sdi}(\psi) \tag{13}$$

where $A(\psi)_i=[c(\psi)+S_sS_a(\psi)]_i$. The system of ordinary differential equations represented by (13) was integrated in time using DASPK [*Brown et al.,* 1994], which is a popular differential algebraic equation integrator based on a fixed-leading-coefficient backward-difference approximation method of variable step size and variable order up to fifth. We have detailed this solution approach and compared efficiency with a variety of standard approaches in recent work [*Tocci et al.,* 1997]. We include this approach for completeness and because the issues of concern in this work apply to both of the temporal discretization methods outlined above.

3.5. Permeability Approximations

An important aspect of this work is the approach used to estimate permeabilities that vary in space as a function of ψ within the spatial discretization scheme. The values of concern appear as $K_{i\pm1/2}$ in (11). Several approaches have been suggested in

the literature [*Haverkamp and Vauclin,* 1979; *Warrick,* 1991; *Zaidel and Russo,* 1992], but a detailed comparison of these approaches in a context similar to this work has not yet appeared. After initial screening of several approaches, we focused on three for a detailed investigation: arithmetic average permeability, integral permeability, and the permeability based upon an arithmetic average of saturation.

A common approach for estimating $K_{i\pm1/2}$ is the arithmetic mean technique (KAM) [*Haverkamp and Vauclin,* 1979; *Warrick,* 1991; *Zaidel and Russo,* 1992]:

$$K_{i\pm1/2} = \left(K_i + K_{i\pm1}\right)/2 \tag{14}$$

which is simple and inexpensive to compute.

Because K varies in space as a function of ψ, an integral representation of mean interblock values (KINT) can be computed as

$$K_{i\pm1/2} = \begin{cases} \frac{1}{|\psi_i - \psi_{i\pm1}|} \int_{\min\{\psi_i,\psi_{i\pm1}\}}^{\max\{\psi_i,\psi_{i\pm1}\}} K\, d\psi, & \text{if } \psi_i \neq \psi_{i\pm1}; \\ K(\psi_i), & \text{if } \psi_i = \psi_{i\pm1}. \end{cases} \tag{15}$$

This approach has appeared in the literature [*Zaidel and Russo,* 1992; *Warrick,* 1991], but has not been routinely used—likely because of the apparent computational expense.

The third method considered for estimating $K_{i\pm1/2}$ is termed the arithmetic mean saturation (KAMS) and is computed by

$$K_{i\pm1/2} = K\left[\left(S_{e_i} + S_{e_{i\pm1}}\right)/2\right] \tag{16}$$

The KAMS approach is easy to compute and has appeared in the literature [*Zaidel and Russo,* 1992].

3.6. Constitutive Relation Estimation

Computing VGM constitutive relations can comprise a significant portion of the computational effort required for simulating RE, primarily because of the number of exponential functions that require evaluation and the relative expense of these

operations. Computational time can be significantly reduced by using cubic spline interpolation of tables computed using direct function evaluations and stored prior to time stepping [*Ross,* 1992; *Tocci et al.,* 1997]. The method used to compute these relations affects the robustness issues that are considered in this work. We consider three approaches for evaluation of these constitutive relations: (1) direct function evaluation; (2) cubic spline interpolation; and (3) Hermite spline interpolation. For the direct evaluation approach, the necessary relations are evaluated as needed during the simulation from the definition of the VGM relations, which is the usual procedure. Cubic spline approximations are computed using the standard approach [*Atkinson,* 1989], yielding exact values at the knots and a C^2 continuous representation of the relations.

The Hermite interpolation method differs from the cubic spline method in that the interpolating function is C^1 continuous, the derivatives at the knots correspond to the actual derivatives of the function, and support for the interpolation expression is local. Local support implies that the interpolated value depends only upon values of the function and its derivative at knots that bound the interval within which it lies. In order to use Hermite interpolation, derivatives of the function must be available, as is the case here. For a given function $f(x)$, the Hermite interpolation may be stated as

$$\hat{f}(x) = N_{01} f_1 + N_{02} f_2 + N_{11} \frac{df_1}{dx} + N_{12} \frac{df_2}{dx} \tag{17}$$

and the derivative of the function assumes the form

$$\frac{d\hat{f}(x)}{dx} = \frac{dN_{01}}{dx} f_1 + \frac{dN_{02}}{dx} f_2 + \frac{dN_{11}}{dx} \frac{df_1}{dx} + \frac{dN_{12}}{dx} \frac{df_2}{dx} \tag{18}$$

where the polynomials N_{ij} are defined such that

$$\frac{d^n N_{ij}}{dx^n} = \begin{cases} 1, & x = x_j, n = i; \\ 0, & x = x_k, n \neq i; \\ 0, & x = x_k, k \neq j. \end{cases} \tag{19}$$

where x_k is the location of knot k.

Based upon the properties described in (19), the polynomial expressions N_{ij} are defined as

$$N_{01}(x) = \frac{1}{2l_x^3}\left[2\left(x-\bar{x}\right)-l_x\right]^2\left[\left(x-\bar{x}\right)+l_x\right] \tag{20}$$

$$N_{02}(x) = -\frac{1}{2l_x^3}\left[2\left(x-\bar{x}\right)+l_x\right]^2\left[\left(x-\bar{x}\right)-l_x\right] \tag{21}$$

$$N_{11}(x) = \frac{1}{8l_x^2}\left[2\left(x-\bar{x}\right)-l_x\right]^2\left[2\left(x-\bar{x}\right)+l_x\right] \tag{22}$$

$$N_{12}(x) = \frac{1}{8l_x^2}\left[2\left(x-\bar{x}\right)+l_x\right]^2\left[2\left(x-\bar{x}\right)-l_x\right] \tag{23}$$

$$\frac{dN_{01}(x)}{dx} = \frac{3}{2l_x^3}\left[2\left(x-\bar{x}\right)+l_x\right]\left[2\left(x-\bar{x}\right)-l_x\right] \tag{24}$$

$$\frac{dN_{02}(x)}{dx} = -\frac{3}{2l_x^3}\left[2\left(x-\bar{x}\right)+l_x\right]\left[2\left(x-\bar{x}\right)-l_x\right] \tag{25}$$

$$\frac{dN_{11}(x)}{dx} = \frac{1}{4l_x^2}\left[6\left(x-\bar{x}\right)+l_x\right]\left[2\left(x-\bar{x}\right)-l_x\right] \tag{26}$$

$$\frac{dN_{12}(x)}{dx} = \frac{1}{4l_x^2}\left[6\left(x-\bar{x}\right)-l_x\right]\left[2\left(x-\bar{x}\right)+l_x\right] \tag{27}$$

where x_1 and x_2 are the spline knots adjacent to x, $\bar{x} = (x_1 + x_2)/2$, and $l_x = x_2 - x_1$.

The advantage of Hermite interpolation for this application is that the error is local, meaing that if $x_j \le x \le x_{j+1}$, then

$$|\hat{f}(x) - f(x)| \le \frac{x_{j+1} - x_j}{384} \max_{x_j \le \xi \le x_{j+1}} |f^{(4)}(\xi)|. \tag{28}$$

This error should be compared with that of the standard cubic spline interpolation

$$|\hat{f}(x) - f(x)| \le \frac{5\max(x_{j+1} - x_j)}{384} \max_{x_0 \le \xi \le x_N} |f^{(4)}(\xi)|. \tag{29}$$

where x_0 and x_N correspond to the end points of the entire interval being splined.

The upper bound of the Hermite interpolation error has an advantage of a factor of 5 in the constant. More significantly, the maximum of the fourth derivative is taken only over the interval of knots containing x. For the problems considered here, this isolates the nonsmooth effects.

3.7. Algebraic Equation Solution

The backward Euler time integration method applied to (1) was solved using a standard modified Picard iteration method to resolve the nonlinearities, which is detailed in the literature [*Celia et al.,* 1990]. The DAE/MOL approach for approximating (2) of DASPK uses a chord iteration method to resolve the nonlinearities, which is also detailed elsewhere [*Tocci et al.,* 1997].

Both approaches result in a tridiagonal system of linear equations that require solution at each iteration. A lower-upper decomposition approach was used to solve this system of equations, with refactoring of the Jacobian matrix, $[J]$, in the DAE/MOL approach only done when $[J]$ was reformed. In previous work, we found that cyclic reduction was a much more efficient method of solving such systems of equations on a high-performance vector machine [*Tocci et al.,* 1997]. The central issues of concern in this work are not affected by the choice of a linear solver.

4. Results and Discussion

4.1. Test Conditions

To meet our objectives, we performed a set of numerical experiments for two time integration methods, three interblock permeability approaches, and three constitutive relation computation methods, detailed above. We applied these method combinations to a set of three test problems representative of widely different natural media, as shown in Table 1.

Table 1

We chose media parameters that correspond to the average values for the loam and clay loam soil textural groups according to the USDA classification [*van Genuchten et al.,* 1991], as well as the sand problem used in our previous work [*Tocci et al.,* 1997]. The loam and clay loam problems are typically difficult to simulate numerically using conventional methods, due to the non-smooth behavior of the resulting permeability

and specific moisture capacity functions. The sand media has a $n_v = 4.264$, so its VGM relations are smooth compared to the loam and clay loam materials. This sand was included to provide a wide range of material properties for the method comparisons so that robustness was evaluated thoroughly.

The material properties and spatial and temporal domain information for the set of test problems listed in Table 1 were used to perform a set of dense-grid simulations, which were used to judge the accuracy of the set of methods considered. The solutions from these dense-grid simulations are shown in Figure 1 and illustrate a sharp infiltration front between an unsaturated and a saturated zone, which is the hallmark of each of the test problems.

Figure 1

4.2. Spline Approximations

The accuracy of the cubic and Hermite spline approximations to the analytical VGM relations was examined for the c and K functions in each medium by varying the number of knots in the approximation between 101 and 10,101 and computing the L_1 norm of the solution error at a set of 40,401 points, which included both knot points and points that fell in an interval between knots. In each case, knots were equally spaced between $\psi = -10.0$ and $\psi = 0.1$. Table 2 shows the slope of log error versus log np, where np is the number of knots, and the L_1 norm of interpolation error at a reference point of 5051 spline knots. The slope of log error versus log np represents the order of the approximation for each of the respective interpolants. For the sand problem, $n_v = 4.264$, the error is of approximately order four, which is the expected result for a third-order polynomial interpolant of a smooth function. However, for the loam and clay loam media, the loss of smoothness is manifested by a much lower order of accuracy in the interpolant. The accuracy decreases as n_v decreases, as is evident in the decreased order of approximation for the clay loam relative to the loam and sand materials.

Table 2

Figures 2–5 compare the actual function and either a cubic or Hermite spline

Figures 2–5

approximation for specific moisture capacity and permeability as a function of the number of knots for the clay loam. These figures illustrate the discontinuity in the derivative of these relations and the nature of the spline errors. The cubic splines are shown to be smooth but oscillatory, which is expected to lead to convergence problems for a nonlinear solver that depends upon derivative information. The Hermite splines are non-oscillatory and smooth, matching exactly the constitutive relation values and the derivative of these constitutive relations at each knot. The Hermite spline approximation has a smoothness and order of continuity that exceeds the constitutive relation being approximated. For an equivalent number of knots and non-smooth relations, Hermite spline interpolation typically has a smaller error than cubic spline interpolation. For the sand media, the constitutive relations are smooth, and both spline approximations provide a very accurate representation of the true solution.

4.3. Work Measures

For methods based upon the MPI approach, the work primarily concerns forming the coefficient matrix and right hand side vector, and solving the linear systems of equations. This observation allows for a simple, straightforward measure of work that requires relative weights for the two procedures and integer counts for each of the procedures, such as

$$W_p = w_c n_c + w_l n_l \tag{30}$$

where W_p is a work measure for MPI methods, w_c is a weighting factor for formation of the coefficient matrix and right hand side vector, which are typically done at the same time, w_l is a weighting factor for solution of the linear system of equations, n_c is the number of coefficient matrix formation calls, and n_l is the number of linear solutions performed [*Tocci et al.,* 1997].

For traditional low-order DAE methods and DAE/MOL approaches that rely upon Newton iteration methods to resolve nonlinearities, the majority of the work is

associated with Jacobian evaluations, function evaluations, and the solution of the linear system of equations. A work measure of the form

$$W_n = w_j n_j + w_f n_f + w_l n_l \tag{31}$$

is produced, where W_n is a work measure for Newton iteration DAE methods, w_j is a weighting factor for formation of the Jacobian matrix, w_f is a weighting factor for evaluation of the function, n_j is the number of Jacobian evaluations, and n_f is the number of function evaluations [*Tocci et al.,* 1997].

The weighting factors will depend on the function evaluation and interblock permeability estimation methods used. Table 3 shows the weighting factors for each of the nine combinations of function evaluation and interblock permeability estimation methods. These weights are based upon a detailed set of profiling results. It is clear from this table that KINT is the most expensive to compute when using direct function evaluation (DFE), but is competitive with KAM when using cubic spline interpolation (CSI) or Hermite spline interpolation (HSI). The KAMS method is less costly than KINT when using DFE but is not as efficient when using a spline interpolation method. This added expense for KAMS when used with a spline interpolation is due to the fact that additional work is required in converting the calculated average saturation to ψ in order to interpolate the constitutive functions which are expressed in terms of ψ.

Table 3

4.4. Simulation Results

Simulations of infiltration into initially dry, non-uniform ($n_v < 2$) media show that the cubic spline interpolation method does not maintain a high enough degree of accuracy to give robust and accurate results. For reasons described above, Hermite polynomial splines are tested in place of cubic splines for constitutive function evaluations. Results also show that the KAM permeability estimation technique is not robust and often fails for problems involving non-uniform media. The KINT and KAMS

techniques were tested as possible robust alternatives to the KAM method.

Tables 4–9 show the work and dense grid errors over a wide range of time step sizes, using both MPI and DASPK solvers for the three test problems. Results are shown for both the direct function evaluation as well as the Hermite spline interpolation methods using three different interblock permeability estimation techniques: KAM, KINT, and KAMS. Tables 4–9

4.5. Solution Efficiency

From the simulation results, it is clear that the KINT and KAMS permeability estimation techniques are more robust than KAM, with KINT giving more accurate results in most cases. Moreover, the variable step size, Newton-type iteration of DASPK performs better than the fixed time step MPI nonlinear solver. For all of the results shown, the Jacobians in DASPK are computed numerically by finite differences.

If one replaces the Picard iteration with a Newton iteration, the robustness of the iteration is enhanced. However, the nonsmoothness means that the Jacobian may not exist. Even if the discretization does not require differentiation at $\psi = 0$, the nonsmooth nonlinearities will reduce the radius of the ball of attraction of the Newton iteration [*Kelley,* 1995]. Hence, a fixed-step method for temporal integration, which does not adjust the time step to account for errors in the integration or slow convergence of the nonlinear solver, could fail even if Newton's method were used as a solver unless a globalization method, such as a line search, [*Dennis and Schnabel,* 1996; *Kelley,* 1995; *Ortega and Rheinboldt,* 1970] were used.

These problems with nonsmoothness also affect the accuracy of approximations to the constitutive laws that are made in the interest of efficiency. The nonlinearities in RE are extremely costly to evaluate, and adding Jacobian evaluations to that cost could well make the computation impractical. Replacing the nonlinearities by spline approximations will significantly improve performance [*Tocci et al.,* 1997], but the

accuracy of these spline approximations is degraded as the nonlinearities become less smooth, which is exactly what happens as n_v is decreased.

As our results verify, the problems caused by small n_v can be solved by a combination of averaging more accurately the permeabilities used in the discrete equations, and approximating Jacobian information in such a way that the Jacobian is more directly related to the smooth problem, rather than approximating the Jacobian for the original, nonsmooth problem. This solution strategy deserves some theoretical consideration. The Newton iterative approach and approximation of the nonlinearity are examined in further detail in the following sections.

4.6. Newton Iteration

If we discretize (2) in space, we obtain a finite dimensional system of ordinary differential equations of the form

$$G(\psi, d\psi/dt) = A(\psi)d\psi/dt + B(\psi) = 0 \tag{32}$$

where $B(\psi)$ is the discretization of the spatial derivative term

$$-\frac{\partial}{\partial z}\left[K_z(\psi)\left(\frac{\partial \psi}{\partial z} + 1\right)\right] \tag{33}$$

Numerical approximation of B with finite differences or finite elements would not require evaluation of the derivative of K_z. Hence the smoothness of the discretized problem is the same as that of the continuous one.

Following [*Tocci et al.,* 1997] and [*Kelley et al.,* 1996], we approach (32) as a differential algebraic equation [*Brenan et al.,* 1996] and do not divide by A. If one integrates implicitly in time, one must solve a nonlinear equation at each time step of the form [*Brenan et al.,* 1996]

$$F(u) = G(u, \alpha u + \beta) = 0 \tag{34}$$

where u will be the approximate solution at the current time step and α and β depend on the parameters of the problem and the history of the integration.

F will be no smoother than A or B. Because of the presence of S_e' in A, the smoothness of F will be no better than that of S_e'. The standard convergence theory for Newton's method [*Dennis and Schnabel,* 1996; *Kelley,* 1995; *Ortega and Rheinboldt,* 1970], requires that F', the Jacobian of F, be Lipschitz continuous, and hence that $n_v \geq 3$. If $2 < n_v < 3$, F' is Hölder continuous, and Newton's method will still converge [*Keller,* 1970] with only the ultimate convergence rate being slower. However, if $1 < n_v \leq 2$, c (and hence A) is not differentiable, and one would expect problems with Newton's method.

4.7. Approximation of the Nonlinearity

One approach to the smoothness issue is simply to approximate the nonlinearities by splines and apply Newton's method to the resulting problem. Two subtle points must be considered:

- the accuracy of the spline approximation will be degraded because of the nonsmoothness; and
- the derivative of spline approximation is not the same as the spline approximation of the derivative.

As we have seen, $A(\psi)$ and $B(\psi)$ are smooth except when ψ is near zero. At $\psi = 0$, both have algebraic behavior like $|\psi|^{n_v - 1}$. Hence, if we define a spline approximation to F by

$$F_S(u) = A_S(u)(\alpha u + \beta) + B_S(u) \tag{35}$$

where A_S and B_S are spline approximations to A and B, we can use the estimates

$$\|A_S - A\|_\infty, \|B_S - B\|_\infty = O(\delta_\psi^{n_v - 1}) \tag{36}$$

where δ_ψ is the mesh spacing for the spline approximations to A and B, to show that, if $F(u^*) = 0$, where u^* is the exact solution, then

$$\|F_S(u^*)\|_\infty = O(\delta_\psi^{n_v - 1}) \tag{37}$$

which can be made as small as spatial/temporal truncation error if δ_ψ is sufficiently small.

We make the conditioning assumption that there is $C_1 > 0$ such that

$$\|F(u)\| = \|F(u) - F(u^*)\| \geq C_1 \|u - u^*\| \tag{38}$$

for u sufficiently near u^*. Equation (38) simply means that small residuals imply small errors.

So if $F_S(w) = 0$ then

$$\|w - u^*\| \leq C_1^{-1} \|F(w) - F(u^*)\| = C_1^{-1} \|F(w) - F_S(w)\| = O(\delta_\psi^{n_v - 1}). \tag{39}$$

Hence, the solution to the splined equations approximates the solution only insofar as the spline is accurate.

At this point we can conclude that if (38) holds and the nonlinear approximate equation is solved to sufficient accuracy, then the errors in the solutions will be of the same order as the errors in the approximate nonlinearity.

As for convergence of the Newton iteration. The standard error estimate says there is C_2 such that

$$\|e_+\| \leq C_2 \gamma \|F_S'(u^*)^{-1}\| \|e_c\|^2 \tag{40}$$

where e_+ is the error in the Newton step, and e_c is the error in the previous Newton step. In (40), γ is the Lipschitz constant of the Jacobian of the spline approximation, which will be large in this case. A large γ may have several consequences.

- A line search may be needed for most of the nonlinear iterations unless the performance of the nonlinear iteration plays a role in the step size control of the temporal integration.

- The Lipschitz constant of the spline-of-derivative will be far larger that that of F_S'. Hence it is necessary to compute Jacobian information using the derivative of the spline. Computing Jacobians by differences will automatically do this. However, if one wishes to use analytic Jacobians, the potential for nonsmoothness must be considered.

- A low-order spline may provide more accuracy than a high-order spline which uses the same knots.

An important benefit of using the KINT/Hermite spline interpolation approach is that it eliminates the need to evaluate $dK_z/d\psi$, even when using analytic Jacobians. In the KINT approach, only the values $\int K_z d\psi$ and K_z need be tabulated at each of the spline knots. From these tabulated values, interblock permeabilities as well as derivatives of interblock permeabilities can be evaluated. This is important when using a Newton iterative nonlinear solver, where derivatives of the interblock permeabilities may be required.

5. Conclusions

In this work, we have introduced a computational approach that more effectively addresses the difficulties involved in solving RE for non-uniform porous media. By using a combination of non-standard techniques, we were able to construct a more robust and accurate solver for variably saturated flow problems. Several key observations from our numerical experiments and analysis guided the development of the improved simulator:

- Due to the non-smooth behavior of the constitutive relations for non-uniform porous media, more accurate interpolation of the constitutive functions is necessary. We found that a Hermite spline interpolation method is more accurate than the standard linear interpolation or cubic spline interpolation methods for

such problems, and thus plays a key role in the development of a robust and efficient variably saturated flow simulator.

- Standard arithmetic averaging of interblock permeabilities is not robust enough for problems involving non-uniform porous media and, as a result, alternate methods were tested. An integral approach as well as an arithmetic average of nodal saturations approach were both found to be effective, with the integral approach being more efficient and accurate.

- The lack of smoothness in non-uniform porous media flow problems often results in failure of the standard Picard iteration methods, yet the robustness of the iterations is enhanced with a Newton iteration. A fixed time step method for temporal integration, which does not adjust the time step to account for errors in the integration or slow convergence of the nonlinear solver, could fail even if Newton's method were used as a solver. But variable time step Newton's method solvers, such as DASPK, give robust, efficient, and accurate results for the type of non-smooth problems examined in this work.

In developing a robust variably saturated flow simulator, we would recommend the use of the methods listed above. The KINT/Hermite interpolation approach combined with a MOL formulation and variable time step DAE solution method can provide the necessary computational accuracy, efficiency and robustness. This approach is fairly simple to implement and allows a wider range of problems to be solved, including a specific class of problems which conventional simulators are not able to address effectively. Unlike conventional methods used in many simulators, this approach results in robust convergence of the nonlinear solver for the type of non-uniform porous media found in many field soils.

Acknowledgments.

This work supported in part by U.S. Army Waterways Experiment Station Contract DACA39-95-K-0098. In addition, the UNC portion of this work was also supported by: Army Research Office Grant DAAL03-92-G-0111, National Institute of Environmental Health Sciences Grant 5 P42 ES05948, and a Department of Energy Computational Science Fellowship. The NCSU part of this research was also supported by National Science Foundation Grants DMS-9321938 and DMS-9700569, a Cray Research Corporation Fellowship, and a U. S. Department of Education GAANN Fellowship. Computing activity was partially supported by allocations from the North Carolina Supercomputing Center.

References

Allen, M. B. and C. L. Murphy, A finite element collocation method for variably saturated flow in two space dimentions, *Wat. Resour. Res., 22*(11), 1537-1542, 1986.

Atkinson, K. E., *An Introduction to Numerical Analysis,* John Wiley and Sons, New York, NY, 1989.

Brenan, K. E., S. L. Campbell, and L. R. Petzold, *The Numerical Solution of Initial Value Problems in Differential-Algebraic Equations,* SIAM Frontiers in Applied Mathematics, vol. 16, SIAM, Philadelphia, PA, 1996.

Brooks, R. H. and A. T. Corey, Properties of porous media affecting fluid flow, *J. Irrig. Drain. Div., Am. Soc. Civil Eng., 92,*(IR2), 61-88, 1966.

Brown, P. N., A. C. Hindmarsh, and L. R. Petzold, Using Krylov methods in the solution of large-scale differential-algebraic systems, *SIAM J. Stat. Comp, 15,* 1467-1488, 1994.

Celia, M. A., E. T. Bouloutas, and R. L. Zarba, A general mass-conservative numerical solution for the unsaturated flow equation, *Wat. Resour. Res., 26,*(7), 1483-1496, 1990.

Christakos, G., *Random Field Models in Earth Sciences,* Academic Press, San Diego, CA, 1992.

Cooley, R. L., A finite-difference method for unsteady flow in variably saturated porous media: Application to a single pumping well, *Wat. Resour. Res., 7*(10), 1607-1625, 1971.

Cooley, R. L., Some new procedures for numerical solution of variably saturated flow problems, *Wat. Resour. Res., 19*(5), 1271-1285, 1983.

Dennis, J. E. and R. B. Schnabel, *Numerical Methods for Unconstrained Optimization and Nonlinear Equations,* SIAM, Philadelphia, PA, 1996.

Forsyth, P. A., Y. S. Wu, and K. Pruess, Robust numerical methods for saturated-unsaturated flow with dry initial conditions in heterogeneous media, *Adv. in Wat. Resour., 18,* 25-38, 1995.

Freeze, R. A., Three-dimensional, transient, saturated-unsaturated flow in a groundwater basin, *Wat. Resour. Res., 7*(2), 347-366, 1971.

Gelhar, L. W., *Stochastic Subsurface Hydrology,* Prentice Hall, Englewood Cliffs, NJ, 1993.

Hanks, R. J. and S. A. Bowers, Numerical solution of the moisture flow equation for infiltration into layered soils, *Soil. Sci. Soc. Proc.,* 530-534, 1962.

Haverkamp, R. and M. Vauclin, A note on estimating finite difference interblock hydraulic conductivity values for transient unsaturated flow problems", *Wat. Resour. Res., 15*(1), 181-187, 1979.

Hornberger, G. M. and I. Remson, Numeric studies of a composite soil moisture ground-water system, *J. Hydrol.,* 707-712", 1969.

Huyakorn, P. S. and G. F. Pinder, *Computational Methods in Subsurface Flow,* Academic Press", Orlando, FL, 1983.

Huyakorn, P. S., S. D. Thomas, and B. M. Thompson, Techniques for making finite elements competitive in modeling flow in variably saturated porous media", *Wat. Resour. Res., 20*(8), 1099-1115, 1984.

Keller, H. B., Newton's method under mild differentiability conditions, *J. Comp. Sys. Sci., 4,* 15-28, 1970.

Kelley, C. T., *Iterative Methods for Linear and Nonlinear Equations,* SIAM Frontiers in Applied Mathematics, vol. 16, SIAM, Philadelphia, PA, 1995.

Kelley, C. T., C. T. Miller, and M. D. Tocci, Termination of Newton/chord iterations and the method of lines, *Tech. Rep. CSRC-TR96-19,* North Carolina State University Center for Research in Scientific Computation, Raleigh, NC, 1996.

Kool, J. B, J. C. Parker, and M. Th. van Genuchten, Determining soil hydraulic properties from one-step outflow experiments by parameter estimation: I. Theory and numerical studies, *Soil Sci. Am. J., 49,* 1348-1354, 1985.

Kool, J. B. and J. C. Parker, Development and evaluation of closed-form expressions for hysteretic soil hydraulic properties, *Wat. Resour. Res., 23*(1), 105-114, 1987.

Lenhard, R. J., J. C. Parker, and J. J. Kaluarachchi, A model for hysteretic constitutive relations governing multiphase flow: 3. Refinements and numerical simulations, *Wat. Resour. Res., 25*(7), 1727-1736, 1989.

de Marsily, G., *Quantitative Hydrogeology: Groundwater Hydrology for Engineers,* Academic Press, San Diego, CA, 1986.

Mayer, A. S. and C. T. Miller, The influence of porous medium characteristics and measurement scale on pore-scale distributions of residual nonaqueous phase liquids, *J. Cont. Hydrol., 11*(3/4), 189-213, 1992.

Milly, P. C. D., A mass-conservative procedure for time-stepping in models of unsaturated flow, *Adv. in Wat. Resour., 8*(3), 32-36, 1985.

Mualem, Y., A new model for predicting the hydraulic conductivity of unsaturated porous media, *Wat. Resour. Res., 12,* 513-522, 1976.

Ortega, G. S. and W. C. Rheinboldt, *Iterative Solution of Nonlinear Equations in Several Variables,* Academic Press, New York, NY, 1970.

Rathfelder, K. and L. M. Abriola, Mass conservative numerical solutions of the head-based Richards' equation, *Wat. Resour. Res., 30*(9), 2579-2586, 1994.

Richards, L. A., Capillary conduction of liquids in porous media, *Physics, 1,* 318-333, 1931.

Ross, P. J., Cubic approximation of hydraulic properties for simulations of unsaturated flow, *Wat. Resour. Res., 28*(10), 2617-2620, 1992.

Rubin, J., Theoretical analysis of two-dimensional, transient flow of water in unsaturated and partly unsaturated soils, *Soil Sci. Soc. Am. Proc., 32*(5), 607-615, 1968.

Schnabel, R. R. and E. B. Richie, Calculation of internodal conductances for unsaturated flow simulations: A comparison, *Soil Sci. Soc. Am. J., 48,* 1006-1010, 1984.

Scott, P. S. and G. J. Farquhar and N. Kouwen, Hysteretic effects on net infiltration, *Soil Sci. Soc. Am. J., 48,* 1006-1010, 1984.

Simunek, J. and M. Th. van Genuchten, The CHAIN_2D Code for Simulating the Two-Dimensional Movement of Water, Heat, and Multiple Solutes in Variably-Saturated

Porous Media, *Tech. Rep. 136,* U.S. Salinity Laboratory, USDA/ARS, Riverside, CA, 1994.

Tocci, M. D., C. T. Kelley, and C. T. Miller, Accurate and economical solution of the pressure-head form of Richards' equation by the method of lines, *Adv. in Wat. Resour., 20*(1), 1-14, 1997.

van der Heidje, P. K. M., Compilation of saturated and unsaturated zone modeling software, *Tech. Rep. EPA/R-96/009,* Robert S. Kerr Environmental Research Laboratory Office of Research and Development U.S. Environmental Protection Agency, Ada, OK, 1996.

van Genuchten, M. Th., A closed-form equation for predicting the hydraulic conductivity of unsaturated soils, *Soil Sci. Am. J., 44,*, 892-898, 1980.

van Genuchten, M. Th., F. J. Leij, and S. R. Yates, The RETC code for quantifying the hydraulic functions of of unsaturated soils, *Tech. Rep. IAG-DW12933934,* U.S. Salinity Laboratory, USDA/ARS, Riverside, CA, 1991.

Vauclin, M., D. Khanji, and G. Vauchad, Experimental and numerical study of a transient, two-dimensional unsaturated-saturated water table recharge problem, *Wat. Resour. Res., 15,* 1089-1101, 1979.

Vogel, T. and M. Cislerova, On the reliability of unsaturated hydraulic conductivity calculated from the moisture retention curve, *Transp. in Por. Med., 3,* 1-15, 1988.

Vogel, T., M. Cislerova, and J. W. Hopmans, Porous media with linearly variable hydraulic properties, *Wat. Resour. Res., 27*(10), 2735-2741, 1991.

Warrick, A. W., Numerical approximations of Darcian flow through unsaturated soil, *Wat. Resour. Res., 27*(6), 1215-1222, 1992.

Yeh, G. T., FEMWATER: A Finite Element Model of Water Flow through Saturated-Unsaturated Porous Media – First Revision, *Tech. Rep. ORNL-5567/R1,* Oak Ridge National Laboratory, Oak Ridge, TN, 1987.

Zaidel, J. and D. Russo, Estimation of finite difference interblock conductivities for simulation of infiltration into initially dry soils, *Wat. Resour. Res., 28,* 2285-2295, 1992.

C. T. Miller and G. A. Williams, Center for Multiphase Research, Department of Environmental Sciences and Engineering, University of North Carolina, Chapel Hill, North Carolina 27516-7400. (e-mail: casey_miller@unc.edu, glenn_williams@unc.edu)

C. T. Kelley and M. D. Tocci, Center for Scientific Computation, Department of Mathematics, North Carolina State University, Raleigh, NC. (e-mail: kelley@math.ncsu.edu, mdtocci@unity.ncsu.edu)

Received _____

Submitted to *Water Resources Research,* xx November 1997.

Figure 1. Dense-grid solutions.

Figure 2. Cubic spline interpolation of specific moisture capacity function for clay loam test problem.

Figure 3. Hermite spline interpolation of specific moisture capacity function for clay loam test problem.

Figure 4. Cubic spline interpolation of permeability function for clay loam test problem.

Figure 5. Hermite spline interpolation of permeability function for clay loam test problem.

Table 1. Test Problem Parameters

Variable	Sand	Loam	Clay Loam
θ_r (—)	0.093	0.078	0.095
θ_s (—)	0.301	0.430	0.410
α_v (1/m)	5.470	3.600	1.900
n_v (—)	4.264	1.560	1.310
K_s (m/day)	5.040	0.250	0.062
S_s (1/m)	1.0e-6	1.0e-6	1.0e-6
z (m)	[0,10.0]	[0,5.0]	[0,2.0]
t (days)	[0,0.18]	[0,2.25]	[0,1.0]
ψ_0 (m)	$-z$	$-z$	$-z$
ψ_1 (m)	0.00	0.00	0.00
ψ_2 (m)	0.10	0.10	0.10
Δz (m)	1.25e-2	1.25e-2	6.25e-3
n_n (—)	801	401	321

Table 2. Spline Approximation Measures

Constitutive Function	Spline Method	Measure	Sand	Loam	Clay Loam
$c(\psi)$	Cubic	Order	4.024	1.566	1.318
		Error	3.94e-5	1.061	1.130
	Hermite	Order	3.996	1.568	1.322
		Error	3.67e-5	0.673	0.761
$K(\psi)$	Cubic	Order	4.069	1.554	1.285
		Error	7.94e-5	0.739	0.771
	Hermite	Order	3.994	1.563	1.294
		Error	7.22e-5	0.469	0.521

Table 3. Work Measure Weighting Factors

Function Evaluation	Interblock Permeability	w_j	w_f	w_c	w_l
DFE	KAM	1.010	0.497	1.161	0.181
	KINT	1.879	0.924	2.395	0.181
	KAMS	1.188	0.584	1.354	0.181
CSI	KAM	0.549	0.270	0.465	0.181
	KINT	0.578	0.284	0.512	0.181
	KAMS	0.787	0.387	0.782	0.181
HPI	KAM	0.552	0.271	0.484	0.181
	KINT	0.596	0.293	0.530	0.181
	KAMS	0.814	0.401	0.820	0.181

Table 4. Sand Test Problem – Direct Function Evaluation

Nonlinear Solver	Interblock Permeability	Δt	Work	$\|E\|_1$	$\|E\|_2$	$\|E\|_\infty$
MPI	KAM	5.0e-4	17092	12.8907	7.4169	4.7064
		5.0e-5	45526	8.7814	6.1551	4.6436
		2.5e-5	69317	8.6890	6.1101	4.6381
		1.5e-5	99849	8.6653	6.0960	4.6368
		1.0e-5	131611	8.6562	6.0901	4.6365
	KINT	5.0e-4	28254	8.8430	6.1756	4.6680
		5.0e-5	88591	4.2435	4.1939	4.1939
		2.5e-5	137667	4.1411	4.0993	4.0993
		1.5e-5	198244	4.0992	4.0542	4.0542
		1.0e-5	267914	4.0767	4.0298	4.0298
	KAMS	5.0e-4	18027	8.9319	6.1762	4.6468
		5.0e-5	53880	4.0885	4.0275	4.0273
		2.5e-5	79849	3.7410	3.6231	3.6220
		1.5e-5	119654	3.5391	3.3897	3.3879
		1.0e-5	154332	3.4118	3.2447	3.2424

Table 4. (continued)

Nonlinear Solver	Interblock Permeability	Δt	Work	$\|E\|_1$	$\|E\|_2$	$\|E\|_\infty$
DASPK	KAM	1.0e-2	23228	83.1108	19.9251	5.0932
		5.0e-3	26145	10.2828	6.3711	4.7463
		1.0e-3	23472	8.3922	5.9377	4.6107
		5.0e-4	24651	7.9797	5.6779	4.5681
		1.0e-4	31260	8.4803	5.9889	4.6196
	KINT	1.0e-2	49676	113.4329	23.4999	5.1793
		5.0e-3	55828	9.3970	6.1553	4.7463
		1.0e-3	46607	2.4794	2.3366	2.3341
		5.0e-4	49134	2.3163	2.1594	2.1561
		1.0e-4	59182	3.6816	3.6294	3.6293
	KAMS	1.0e-2	26984	118.7739	24.0513	5.1933
		5.0e-3	30538	35.0706	12.6405	4.9467
		1.0e-3	29673	2.1775	1.8648	1.8510
		5.0e-4	30577	1.0749	0.6771	0.5876
		1.0e-4	39143	2.6761	2.4154	2.4082

Table 5. Loam Test Problem – Direct Function Evaluation

Nonlinear Solver	Interblock Permeability	Δt	Work	$\|E\|_1$	$\|E\|_2$	$\|E\|_\infty$
MPI	KAM	3.0e-3	DNC	···	···	···
		1.0e-3	DNC	···	···	···
		5.0e-4	DNC	···	···	···
		1.0e-4	DNC	···	···	···
		5.0e-5	DNC	···	···	···
	KINT	3.0e-3	45036	0.6427	0.4651	0.4459
		1.0e-3	73975	0.5052	0.3451	0.3053
		5.0e-4	118949	0.4749	0.3204	0.2713
		1.0e-4	455630	0.4524	0.3033	0.2448
		5.0e-5	767328	0.4497	0.3014	0.2415
	KAMS	3.0e-3	23667	1.9572	1.4237	1.3775
		1.0e-3	37578	2.8970	1.9828	1.8369
		5.0e-4	57449	3.1927	2.1246	1.9027
		1.0e-4	177339	3.4562	2.2459	1.9366
		5.0e-5	302232	3.4911	2.2620	1.9399

Table 5. (continued)

Nonlinear Solver	Interblock Permeability	Δt	Work	$\|E\|_1$	$\|E\|_2$	$\|E\|_\infty$
DASPK	KAM	1.0e-2	4619	9.4291	4.1820	2.3769
		5.0e-3	4346	8.2950	3.8612	2.3449
		1.0e-3	4539	2.7161	1.9053	1.8054
		5.0e-4	5675	2.5033	1.8161	1.7461
		1.0e-4	8531	2.3713	1.7593	1.7045
	KINT	1.0e-2	8999	4.2056	2.5194	2.2115
		5.0e-3	9634	4.2789	2.5554	2.2077
		1.0e-3	9700	0.5785	0.4895	0.4885
		5.0e-4	10432	0.5318	0.3520	0.3116
		1.0e-4	14972	0.4374	0.3016	0.2566
	KAMS	1.0e-2	6008	6.2092	3.2547	2.3296
		5.0e-3	6009	4.4514	2.6061	2.2311
		1.0e-3	6489	3.1126	2.0976	1.8982
		5.0e-4	8155	3.6870	2.3495	1.9521
		1.0e-4	12247	3.6393	2.3286	1.9495

Table 6. Clay Loam Test Problem – Direct Function Evaluation

Nonlinear Solver	Interblock Permeability	Δt	Work	$\|E\|_1$	$\|E\|_2$	$\|E\|_\infty$
MPI	KAM	5.0e-3	DNC	···	···	···
		2.0e-3	DNC	···	···	···
		1.0e-3	DNC	···	···	···
		5.0e-4	DNC	···	···	···
		1.0e-4	DNC	···	···	···
	KINT	5.0e-3	17540	0.3271	0.0792	0.0340
		2.0e-3	29086	0.1622	0.0383	0.0146
		1.0e-3	DNC	···	···	···
		5.0e-4	DNC	···	···	···
		1.0e-4	DNC	···	···	···
	KAMS	5.0e-3	DNC	···	···	···
		2.0e-3	11166	1.3230	0.3830	0.1758
		1.0e-3	15705	1.4091	0.4092	0.1896
		5.0e-4	23591	1.4697	0.4284	0.1994
		1.0e-4	78491	1.5455	0.4530	0.2155

Table 6. (continued)

Nonlinear Solver	Interblock Permeability	Δt	Work	$\|E\|_1$	$\|E\|_2$	$\|E\|_\infty$
DASPK	KAM	1.0e-2	DNC	...	...	...
		5.0e-3	1065	0.7014	0.1902	0.0871
		1.0e-3	661546	0.2222	0.0676	0.0339
		5.0e-4	320562	0.3729	0.1050	0.0502
		1.0e-4	195167	0.2694	0.0768	0.0370
	KINT	1.0e-2	1440	0.4413	0.1371	0.0743
		5.0e-3	1682	0.2846	0.0679	0.0265
		1.0e-3	2703	0.0525	0.0127	0.0067
		5.0e-4	3089	0.0740	0.0191	0.0105
		1.0e-4	5139	0.0889	0.0234	0.0120
	KAMS	1.0e-2	1264	2.1833	0.6096	0.2671
		5.0e-3	1705	1.7322	0.5104	0.2384
		1.0e-3	2624	1.8202	0.5281	0.2428
		5.0e-4	3106	1.6998	0.4932	0.2265
		1.0e-4	6146	1.6613	0.4883	0.2267

Table 7. Sand Test Problem – Hermite Spline Interpolation

Nonlinear Solver	Interblock Permeability	Δt	Work	$\|E\|_1$	$\|E\|_2$	$\|E\|_\infty$
MPI	KAM	5.0e-4	8469	12.8907	7.4169	4.7064
		5.0e-5	22559	8.7814	6.1551	4.6436
		2.5e-5	34348	8.6890	6.1101	4.6381
		1.5e-5	49477	8.6653	6.0960	4.6368
		1.0e-5	65217	8.6562	6.0901	4.6365
	KINT	5.0e-4	7798	8.8430	6.1756	4.6680
		5.0e-5	24452	4.2435	4.1939	4.1939
		2.5e-5	37998	4.1411	4.0993	4.0993
		1.5e-5	54717	4.0992	4.0542	4.0542
		1.0e-5	73947	4.0767	4.0298	4.0298
	KAMS	5.0e-4	11756	8.9319	6.1762	4.6468
		5.0e-5	35136	4.0885	4.0275	4.0273
		2.5e-5	52071	3.7410	3.6231	3.6220
		1.5e-5	78029	3.5391	3.3897	3.3897
		1.0e-5	100643	3.4118	3.2447	3.2424

Table 7. (continued)

Nonlinear Solver	Interblock Permeability	Δt	Work	$\|E\|_1$	$\|E\|_2$	$\|E\|_\infty$
DASPK	KAM	1.0e-2	13085	89.2186	20.6225	5.1229
		5.0e-3	15758	6.3996	4.8201	4.7335
		1.0e-3	14011	7.9438	5.6551	4.5639
		5.0e-4	14707	7.9596	5.6653	4.5664
		1.0e-4	18581	8.4843	5.9911	4.6200
	KINT	1.0e-2	18032	116.1722	23.7168	5.1933
		5.0e-3	18806	10.0713	6.5421	4.7463
		1.0e-3	16637	2.2181	2.0551	2.0514
		5.0e-4	17472	2.2511	2.0884	2.0848
		1.0e-4	20892	3.7039	3.6520	3.6518
	KAMS	1.0e-2	18999	125.2336	24.7315	5.2186
		5.0e-3	22694	7.2105	5.0786	4.7463
		1.0e-3	21003	1.3033	0.9120	0.8582
		5.0e-4	22149	1.1793	0.7797	0.7099
		1.0e-4	27906	2.5880	2.3169	2.3087

Table 8. Loam Test Problem – Hermite Spline Interpolation

Nonlinear Solver	Interblock Permeability	Δt	Work	$\|E\|_1$	$\|E\|_2$	$\|E\|_\infty$
MPI	KAM	3.0e-3	DNC	···	···	···
		1.0e-3	DNC	···	···	···
		5.0e-4	DNC	···	···	···
		1.0e-4	DNC	···	···	···
		5.0e-5	DNC	···	···	···
	KINT	3.0e-3	12409	0.6439	0.4653	0.4463
		1.0e-3	20411	0.5035	0.3452	0.3056
		5.0e-4	33167	0.4732	0.3205	0.2716
		1.0e-4	127186	0.4507	0.3033	0.2450
		5.0e-5	213841	0.4480	0.3014	0.2417
	KAMS	3.0e-3	15442	1.9319	1.4076	1.3628
		1.0e-3	24456	2.8686	1.9709	1.8306
		5.0e-4	37499	3.1834	2.1131	1.8991
		1.0e-4	115686	3.4540	2.2334	1.9343
		5.0e-5	197343	3.4896	2.2495	1.9377

Table 8. (continued)

Nonlinear Solver	Interblock Permeability	Δt	Work	$\|E\|_1$	$\|E\|_2$	$\|E\|_\infty$
DASPK	KAM	1.0e-2	2699	6.3299	3.2464	2.2529
		5.0e-3	2769	6.8402	3.4371	2.2884
		1.0e-3	2789	3.0170	2.0291	1.8723
		5.0e-4	3276	2.3804	1.7706	1.7133
		1.0e-4	4674	2.4029	1.7790	1.7191
	KINT	1.0e-2	3199	5.5212	3.0514	2.2954
		5.0e-3	3291	5.1922	2.9363	2.2811
		1.0e-3	3438	0.4386	0.3452	0.3359
		5.0e-4	3662	0.5492	0.3656	0.3289
		1.0e-4	5326	0.4380	0.3008	0.2523
	KAMS	1.0e-2	4305	10.1117	4.4256	2.4252
		5.0e-3	4389	7.7081	3.7520	2.3826
		1.0e-3	4693	3.4169	2.2202	1.9300
		5.0e-4	5137	3.7832	2.3782	1.9551
		1.0e-4	8513	3.5271	2.2665	1.9411

Table 9. Clay Loam Test Problem – Hermite Spline Interpolation

Nonlinear Solver	Interblock Permeability	Δt	Work	$\|E\|_1$	$\|E\|_2$	$\|E\|_\infty$
MPI	KAM	5.0e-3	DNC	···	···	···
		2.0e-3	DNC	···	···	···
		1.0e-3	DNC	···	···	···
		5.0e-4	DNC	···	···	···
		1.0e-4	DNC	···	···	···
	KINT	5.0e-3	4839	0.3270	0.0792	0.0341
		2.0e-3	8044	0.1622	0.0383	0.0146
		1.0e-3	DNC	···	···	···
		5.0e-4	DNC	···	···	···
		1.0e-4	DNC	···	···	···
	KAMS	5.0e-3	5114	1.0725	0.3086	0.1365
		2.0e-3	7301	1.3171	0.3811	0.1749
		1.0e-3	10720	1.4018	0.4068	0.1885
		5.0e-4	15445	1.4635	0.4264	0.1984
		1.0e-4	51460	1.5382	0.4507	0.2104

Table 9. (continued)

Nonlinear Solver	Interblock Permeability	Δt	Work	$\|E\|_1$	$\|E\|_2$	$\|E\|_\infty$
DASPK	KAM	1.0e-2	1042	0.3528	0.0917	0.0400
		5.0e-3	693	0.4130	0.1112	0.0487
		1.0e-3	2419	0.2830	0.0779	0.0346
		5.0e-4	2013	0.1610	0.0543	0.0283
		1.0e-4	4085	0.3381	0.0938	0.0444
	KINT	1.0e-2	511	0.4367	0.1348	0.0732
		5.0e-3	577	0.1975	0.0483	0.0185
		1.0e-3	956	0.0489	0.0095	0.0050
		5.0e-4	1110	0.0670	0.0172	0.0096
		1.0e-4	1765	0.0891	0.0231	0.0119
	KAMS	1.0e-2	912	7.6039	1.9141	0.7255
		5.0e-3	1212	1.5417	0.4528	0.2181
		1.0e-3	1964	2.0917	0.6104	0.2746
		5.0e-4	2515	1.7810	0.5149	0.2374
		1.0e-4	5162	1.6957	0.4988	0.2322

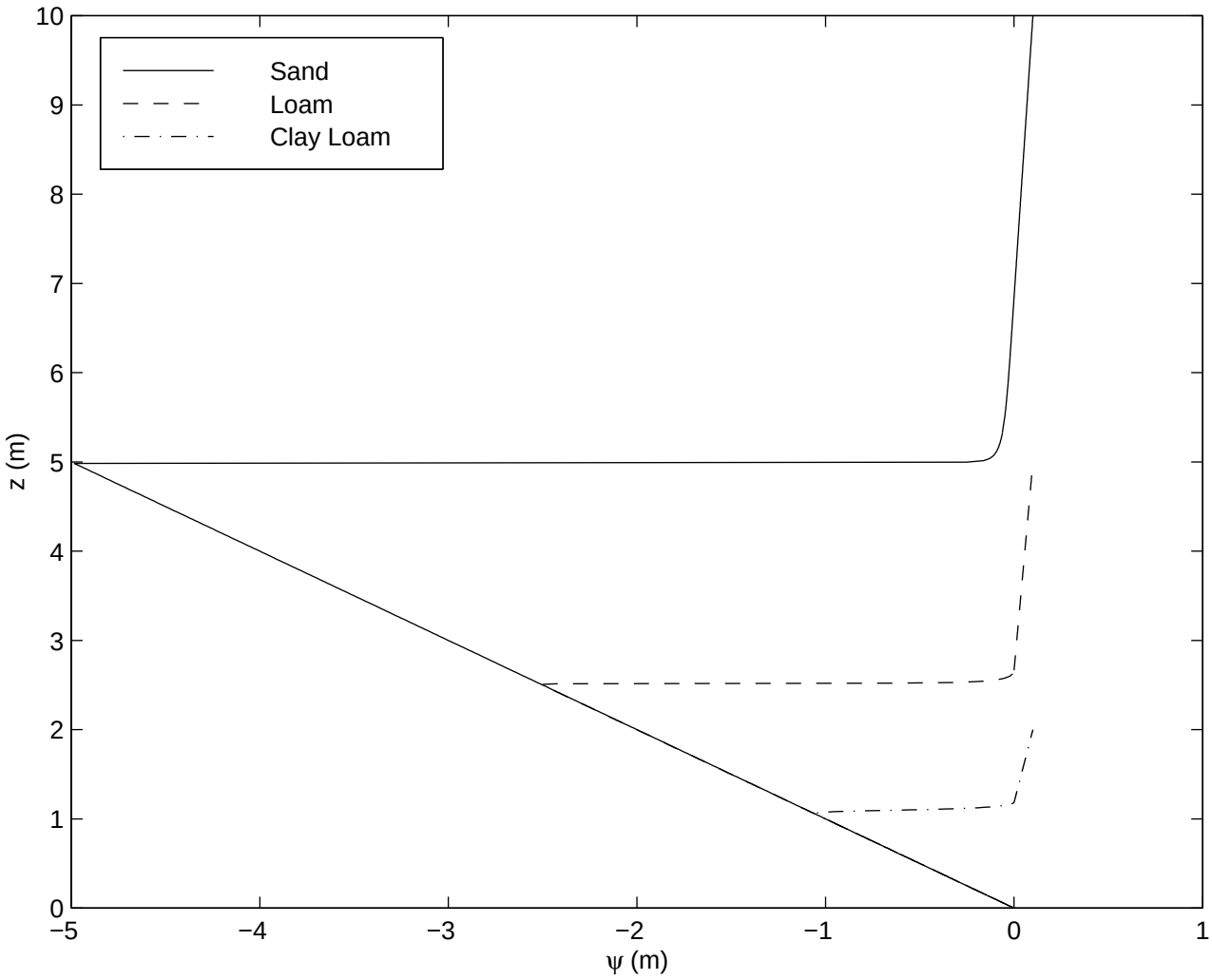
Sand
Loam
Clay Loam
z (m)
ψ (m)
10
9
8
7
6
5
4
3
2
1
0
−5
−4
−3
−2
−1
0
1

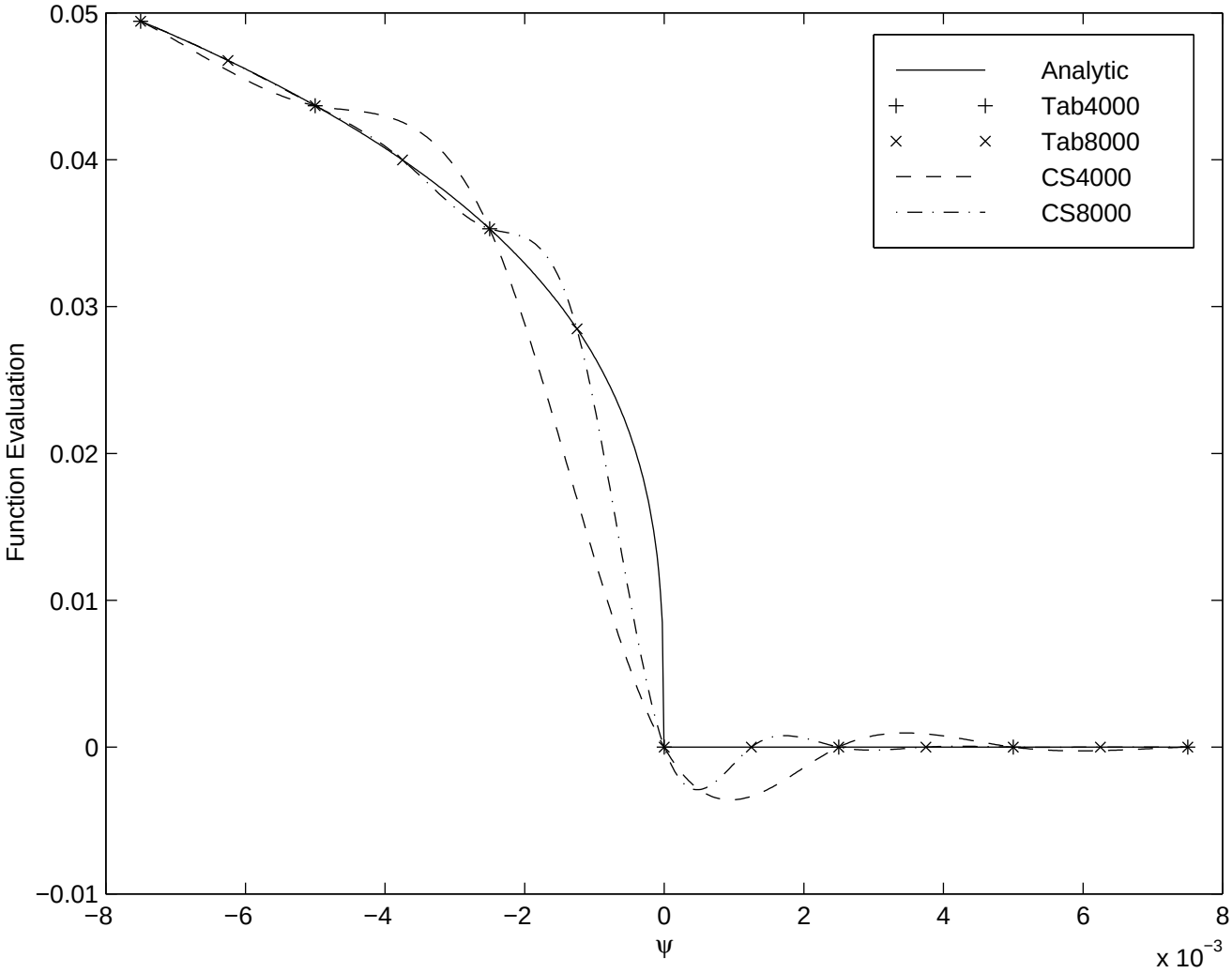
Analytic
Tab4000
Tab8000
CS4000
CS8000
Function Evaluation
ψ
x 10^−3
0.05
0.04
0.03
0.02
0.01
0
−0.01
−8
−6
−4
−2
0
2
4
6
8

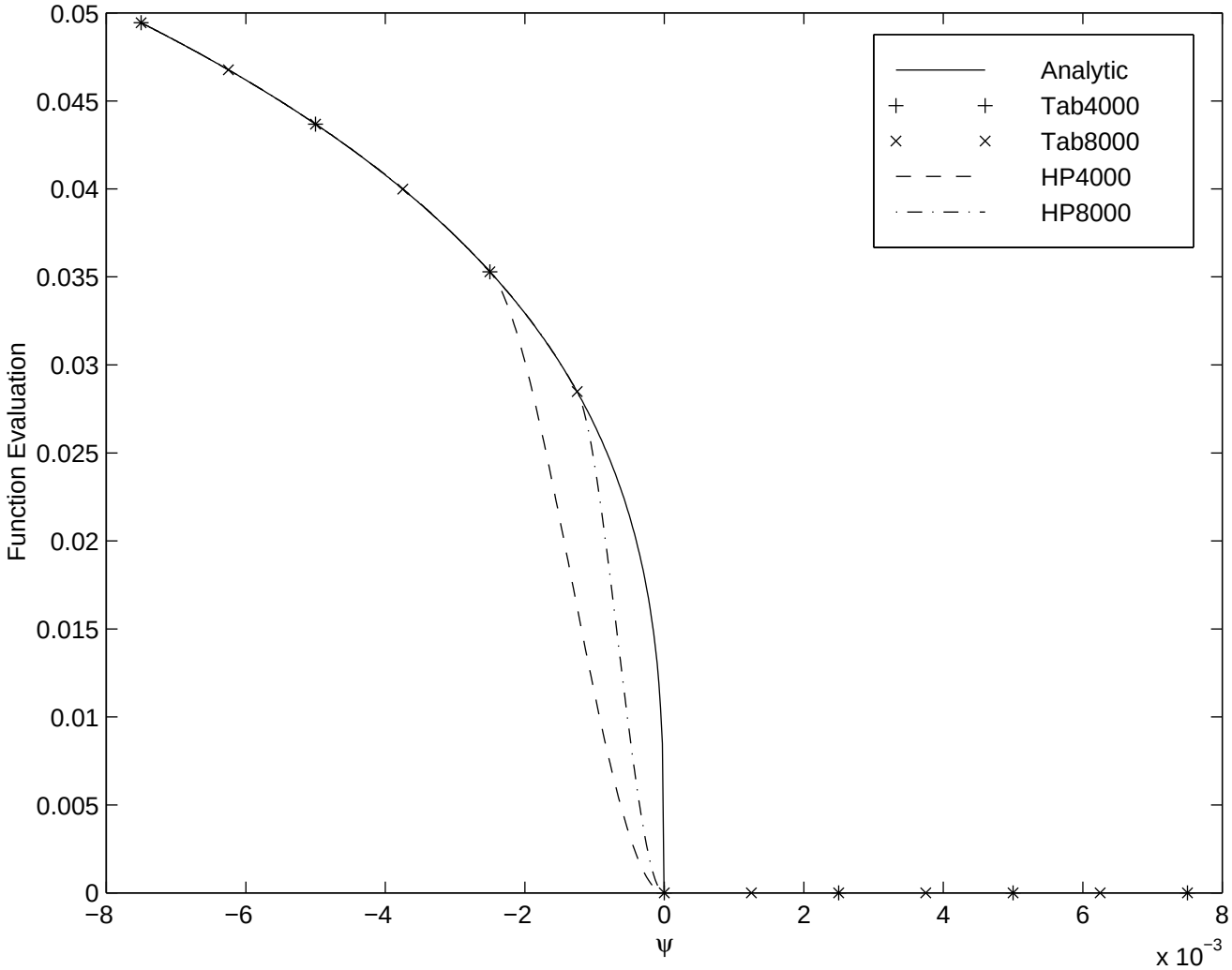
Analytic
Tab4000
Tab8000
HP4000
HP8000
Function Evaluation
0.05
0.045
0.04
0.035
0.03
0.025
0.02
0.015
0.01
0.005
0
−8
−6
−4
−2
0
2
4
6
8
ψ
x 10^−3

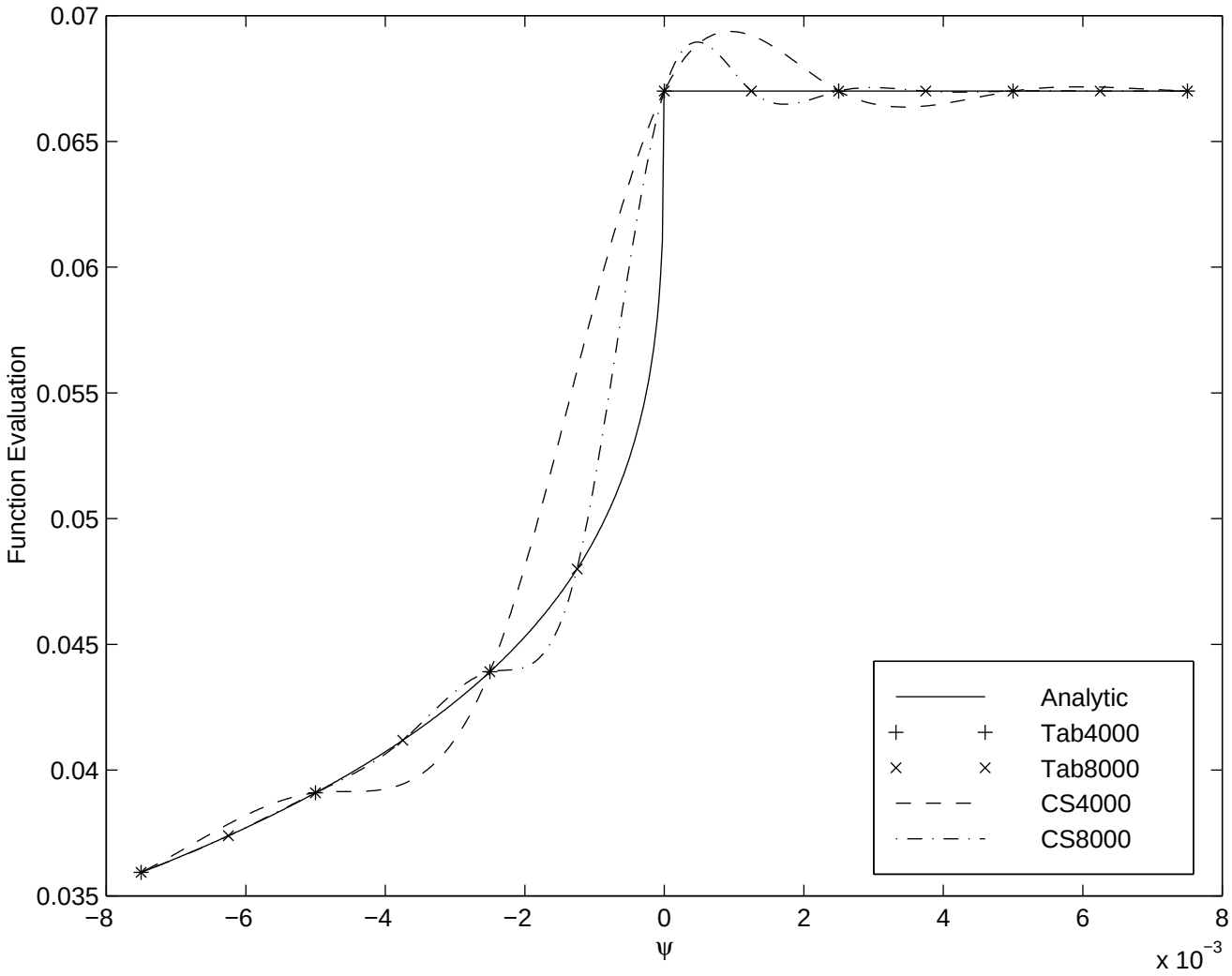
0.07
0.065
0.06
0.055
0.05
0.045
0.04
0.035
Function Evaluation
−8
−6
−4
−2
0
2
4
6
8
ψ
x 10^−3
Analytic
Tab4000
Tab8000
CS4000
CS8000

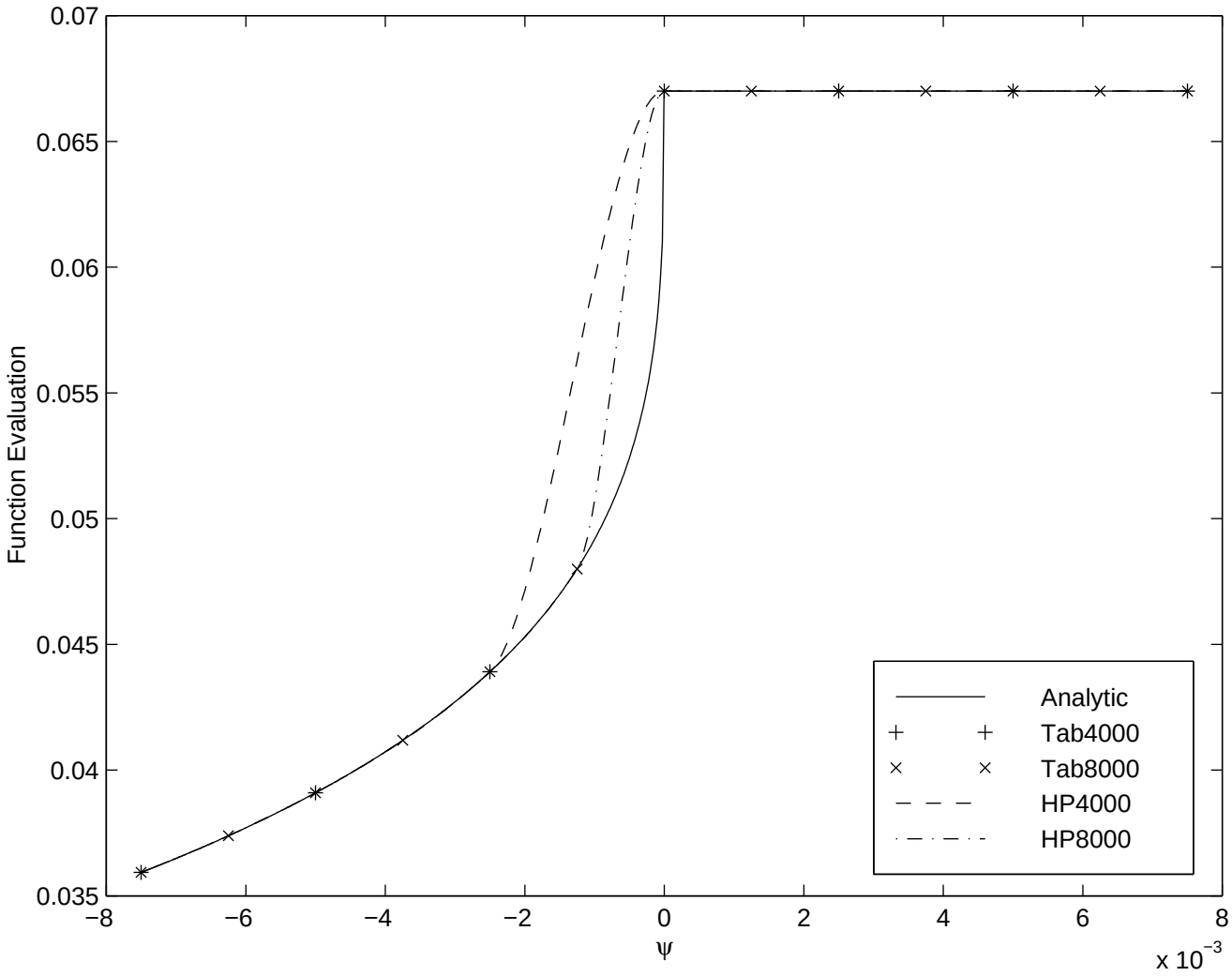
0.07
0.065
0.06
0.055
0.05
0.045
0.04
0.035
Function Evaluation
−8
−6
−4
−2
0
2
4
6
8
ψ
x 10^−3
Analytic
Tab4000
Tab8000
HP4000
HP8000